NANO LETTERS

2007
Vol. 7, No. 2
484−489

Self-Assembled Multilayers of Nanocomponents

R. S. Krishnan,[†] Michael E. Mackay,[*,†,‡] Phillip M. Duxbury,[‡] Alicia Pastor,[§] Craig J. Hawker,[||,⊥] Brooke Van Horn,[⊥] Subashini Asokan,[⊗] and Michael S. Wong[#,⊗]

Department of Chemical Engineering & Materials Science, Michigan State University, East Lansing, Michigan 48824, Department of Physics and Astronomy, Michigan State University, East Lansing, Michigan 48824, Center for Advanced Microscopy, Michigan State University, East Lansing, Michigan 48824, Materials Research Laboratory, University of California, Santa Barbara, California 93106, IBM Almaden Research Center, 650 Harry Road, San Jose, California 95120, Department of Chemical and Biomolecular Engineering, Rice University, Houston, Texas 77251, and Department of Chemistry, Rice University, Houston, Texas 77251

Received December 7, 2006; Revised Manuscript Received December 22, 2006

ABSTRACT

We show it is possible to assemble nanoparticle−polymer layers in a controllable manner dictated by the difference in nano-object morphology and dielectric properties. A thin (10–100 nm) layer of the two components is spin coated onto a solid substrate and the system thermally aged to activate a cross-linking process between polymer molecules. The nanoparticles segregate to the solid substrate prior to complete cross-linking if entropic forces are dominant or to the air interface if dielectric (surface energy) forces are properly tuned. Subsequent layers are then spin coated onto the layer below, and the process is repeated to create layered structures with nanometer accuracy useful for tandem solar cells, sensors, optical coatings, etc. Unlike other self-assembly techniques the layer thicknesses are dictated by the spin coating conditions and relative concentration of the two components.

Self-assembled, ultrathin films function as membranes and sensors as well as photovoltaic devices and structural elements, exemplifying their ubiquitous nature and application.[1−8] Layered self-assembly of amphiphilic materials using the Langmuir−Blodgett procedure[9] is well-known, and more recently electrostatically driven layer-by-layer or LbL assembly of polymeric multicomposites[10,11] has been demonstrated. In the LbL approach the fabrication of polymeric multilayers is achieved by consecutive adsorption of polyanions and polycations and hence is driven by electrostatic forces to achieve monolayers whose thickness is dictated by the polymer geometry. Extension of the LbL method to self-assembly of alternating layers of polymers and nanoparticles significantly extends the scope of this approach.[12] However, the LbL approach cannot be used for nonpolar or uncharged nanoparticles and polymers, which excludes a wide range of functional materials. Here we show that self-assembly of nonpolar linear polymers and nanoparticles into layers with controllable thickness can be fully realized using relatively simple and robust processing steps. Moreover, by controlling entropic and enthalpic driving forces, we demonstrate controlled self-assembly of nanocomponent multilayers, promoting facile manufacture of a wide range of biomimetic[13] and other fascinating[14] nanostructures from nonpolar materials.

Self-assembly of nonpolar, uncharged polymers and nanoparticles is strongly influenced by entropic effects; however local enthalpic terms and long-range dispersion forces can also be significant. Kinetic effects such as jamming and self-assembly during drying are also important in some situations effectively trapping the structures.[15−17] We first show that entropic effects due to architecture differences[18] can drive self-assembly of multilayers by using unique polystyrene nanoparticle−linear polystyrene mixtures where the difference in monomer−monomer enthalpic effects is minimized. Here the nanoparticles assemble at the solid substrate without jamming to maximize the system entropy. We then show that multilayers formed from CdSe quantum dots and linear polystyrene are controlled by the interplay between surface energy, dispersion forces, and entropy. In this system, the nanoparticles primarily segregate to the air interface, yet

* Corresponding author. E-mail: mackay@msu.edu, www.nanoeverything.com
[†] Department of Chemical Engineering & Materials Science, Michigan State University.
[‡] Department of Physics and Astronomy, Michigan State University.
[§] Center for Advanced Microscopy, Michigan State University.
[||] Materials Research Laboratory, University of California.
[⊥] IBM Almaden Research Center.
[#] Department of Chemical and Biomolecular Engineering, Rice University.
[⊗] Department of Chemistry, Rice University.

10.1021/nl062866u CCC: $37.00
Published on Web 01/30/2007

multilayer fabrication remains facile. A third example consists of a multilayer of two incompatible polymers, namely, linear polystyrene and linear poly(methyl methacrylate) (PMMA), where CdSe quantum dots are used to stabilize the multilayer, displaying the capability of our processing technique to incorporate a wide range of polymer and nanoparticle combinations. We also show that different sized nanoparticles segregate into two layers pushing the larger nanoparticles to the solid substrate demonstrating the technique can be used with architecturally and chemically dissimilar systems as well as with systems with chemical similarity but size dissimilarity.

We have recently shown,[19] using neutron reflectivity experiments, that polystyrene nanoparticles made by an intramolecular collapse strategy[20,21] blended with linear polystyrene are uniformly distributed in a spuncast thin film (ca. 40 nm thick). Yet, after annealing the film above the glass transition temperature of the linear polymer, they were found to segregate to the solid substrate. Separate experiments with different deuteration contrast ruled out migration of nanoparticles due to any isotopic effect.[22,23] Also, since the nanoparticles and linear polymer have identical repeat units (styrene monomer), adverse monomeric enthalpic interactions between the linear polymer and the nanoparticles are minimal,[24] the migration of the nanoparticles to the solid substrate is primarily an entropic effect.[25] Nanoparticle localization to an interface[26,27] has great utility since it changes a range of physical and mechanical properties of thin films; in particular it inhibits their dewetting from low-energy substrates,[19,28−30] a phenomenon we use in the present work.

Two prerequisites for facile control of multilayer fabrication are the ability to uniformly disperse nanoparticles in thin films[19] and then to control their segregation to either the substrate or air surface. We first show that a thin film initially composed of a uniform mixture of polystyrene nanoparticles and polystyrene may be annealed to form a bilayer consisting of a nanoparticle-rich phase at the solid substrate and a polymer-rich phase at the air interface. We then show that this process may be repeated, enabling proficient and well-controlled fabrication of multilayers, and that similar processing may be used for a wide range of nanoparticle and polymer combinations. We call this the self-assembled multilayers of nanocomponents or SAMON process.

The process of entropy-driven enrichment of polystyrene nanoparticles at the silicon wafer substrate is demonstrated in Figure 1a where neutron reflectivity measurements (RQ^4 vs Q, R is the reflectance and Q is the wave vector) on a polymer film containing 10 wt % polystyrene nanoparticles (211 kDa) blended with deuterated linear polystyrene (63 kDa) show a distinct change before and after annealing (we clarify if the polymer or nanoparticle contains deuterium by stating it is deuterated, if no isotopic substitution is made then no mention of hydrogen content is made). The completely deuterated linear polystyrene was purchased from Scientific Polymer Products, and the polystyrene nanoparticles were made by collapsing and cross-linking a random copolymer of 20 mol % benzylcyclobutane (BCB) and 80 mol % styrene as discussed by Harth et al.[20] Before being annealed, the ca. 40 nm thick film, which was spin-coated from a benzene solution, was accurately modeled as a single layer with a homogeneous nanoparticle distribution corresponding to an average scattering length density (SLD) of 5.92×10^{-6} Å^{-2}; the solid line in the figure demonstrates the goodness of the fit to the data. Here the SLD of the pure deuterated polymer and that of the nanoparticle is 6.42×10^{-6} Å^{-2} and 1.41×10^{-6} Å^{-2}, respectively. The reflectivity profile undergoes a profound change after annealing for 2 h at 160 °C as demonstrated by the data presented in Figure 1a along with the results of using a two-layer model with a nanoparticle-rich layer at the solid substrate. Note the nanoparticle surface coverage is approximately one-half a monolayer in this example, as determined by a simple mass balance assuming that all the nanoparticles are located at the substrate,[19] as confirmed by the reflectivity measurement.

The solid line in Figure 1a corresponds to a model where the top layer consists of the pure deuterated linear polymer and the bottom layer contains a combination of the deuterated linear polymer and the nanoparticles with an interface roughness of 5 nm comparable to the nanoparticle diameter ($2a$) of approximately 8.8 nm. The results of using an alternative model where the nanoparticles segregate to the air interface yields the dotted line in Figure 1a. These data and further analysis, using a range of models, clearly indicate that the nanoparticles migrate to the solid substrate after high-temperature annealing. This is further illustrated in Figure 1b, where the concentration profile of the annealed film has been extracted from the reflectivity data. A scaled representation of the nanoparticle is also shown in the lower right-hand corner of this figure.

To fabricate multiple polymer−nanoparticle layers, stacked on top of each other, functionalization and cross-linking of each layer were accomplished by spin coating an 85 wt % polymer−15 wt % nanoparticle blend on top of a previously aged and cross-linked film via the procedure shown in Figure 1c. The numbers ①, ②, etc. in the figure represent addition of a new layer. The polymer was a 211 kDa random copolymer of 80 mol % styrene and 20 mol % BCB stabilized from dissolution during the subsequent spin coating operation by heating to 230 °C for 24 h to activate the cross-linking process between BCB groups. Subsequent experiments demonstrated a significantly decreased aging time is actually required. The 78 kDa partially deuterated, cross-linked polystyrene nanoparticles are found to segregate to the substrate or cross-linked polymer layer below prior to completion of the cross-linking process, allowing repetition of this procedure two more times to give a six layer system with each bilayer being about 44 nm in thickness. Note the nanoparticles were synthesized according to the procedure previously described[20] except the styrene monomer was deuterated while the BCB was not. The segregation was confirmed by neutron reflectivity measurements (Figure 1d), where modeling confirmed six layers, demonstrated by the inset, with the nanoparticles at the solid substrate in each bilayer. Modeling the nanoparticle distribution as if they were

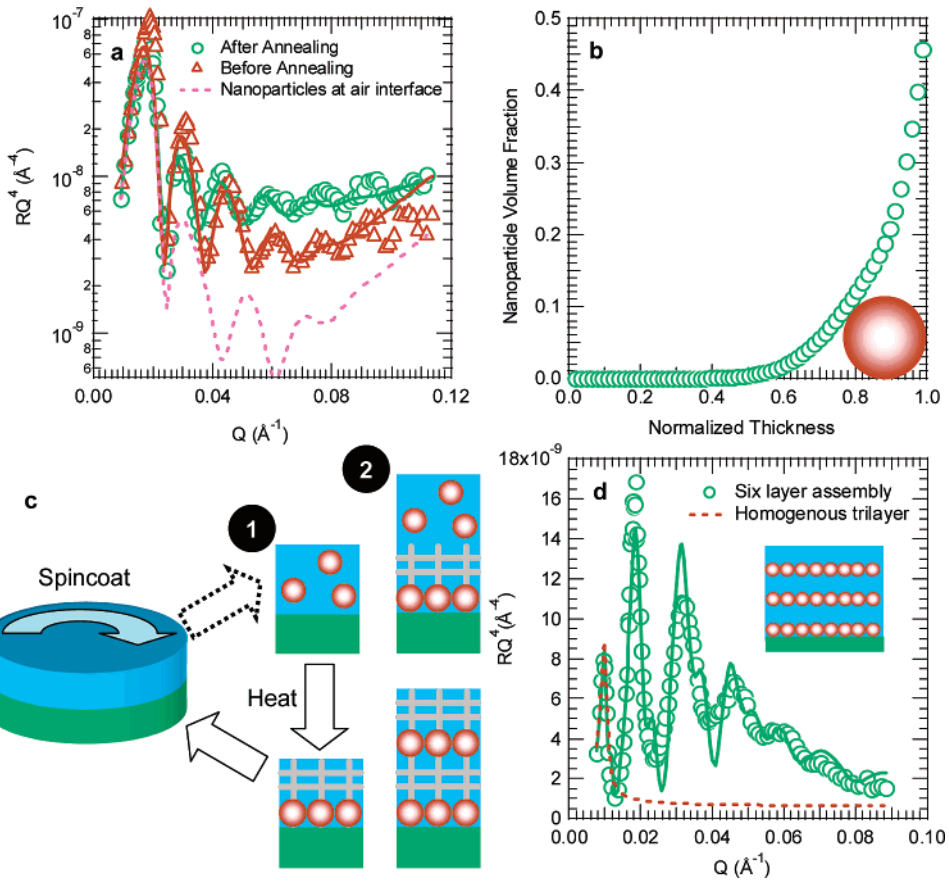

Figure 1. (a) Reflectivity (R) multiplied by reflectance wave vector (Q) to the fourth power (RQ^4) vs Q for a silicon wafer with a thin film (~40 nm) of polymer−nanoparticle mixture before and after annealing to demonstrate that polystyrene nanoparties migrate to the solid substrate. The solid lines represent the fits for the before and after annealed films as described in the text while the dotted line represents the reflectivity profile if the nanoparticles migrated to the air interface. (b) Nanoparticle concentration profile determined from the scattering density profile for the "after annealing" film shown in (a). A scaled representation of the nanoparticle is placed in the lower right-hand corner. (c) Spin-coating process to make the multilayered films. (d) RQ^4 vs Q for a silicon wafer spin coated with three layers of cross-linked polystyrene and polystyrene nanoparticles. The fit (solid line) corresponds to six alternating layers of polymer and deuterated nanoparticle (see inset) while the dotted line is the prediction if the nanoparticles were homogeneously distributed. The thickness of each polymer−nanoparticle layer is approximately 44 nm.

homogeneously distributed shown by the dotted line in the figure, or at the air interface (not shown), gives a poor fit to the data showing that the neutron reflectivity data strongly support the nanoparticle segregation illustrated in the inset.

In this system segregation of the nanoparticles is driven by an entropy gain for the entire system which has been shown to be important when cracks form in nanoparticle filled polymers.[31] Yet, one expects a translational entropy loss when a nanoparticle segregates to the substrate, which is approximately k_BT per nanoparticle, where k_B is Boltzmann's constant and T is temperature. We also found in our previous work[24] that each nanoparticle gains approximately $[a/\sigma]^2 \times \epsilon$ worth of enthalpic contact energy between the nanoparticle and polymer when it is dispersed in the polymer. Here ϵ is the components' monomeric interaction energy and σ is the monomer size, so the nanoparticle loses both enthalpic contacts with the polymer chains and translational entropy due to segregation. This loss is countered by the conformational entropy gain of moving the linear polystyrene chains away from the substrate. An estimate of this entropy gain is $\alpha k_BT[a/\sigma]$,[3] with α representing the degrees of freedom gained by a monomer unit when it is released from substrate constraints. In writing this term, we note that the conformational entropy gain of the linear chain on moving away from the substrate is proportional to the volume of the nanoparticle, a result which is valid provided the nanoparticle is smaller than the radius of gyration of the linear chains. In order for segregation to occur, the conformational entropy gain of the polymer should be greater than the translation entropy and mixing enthalpy losses of the nanoparticle or

$$\alpha\,[a/\sigma]^3 > 1 + [a/\sigma]^2 \times \epsilon/k_BT$$

where ϵ/k_BT is of order 0.1−1 for dispersion forces. Since a and σ are of order 1−10 and 0.1 nm, respectively, then α must be greater than order 0.01−0.1 to allow this segregation. This is reasonable, since a monomer unit on a linear chain may gain up to one degree of freedom on constraint release, in which case $\alpha = 1$.

The versatility of this process is further demonstrated by the ability to replace the polystyrene nanoparticles with inorganic-based materials. Though the above entropic and enthalpic terms are always important in nanoparticle segrega-

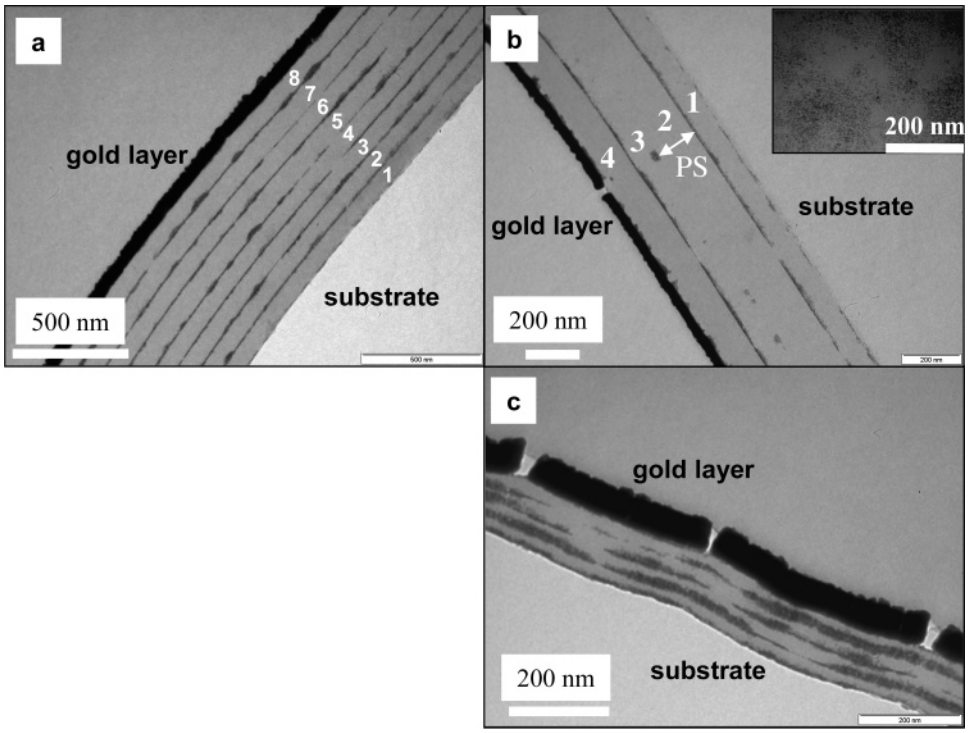

Figure 2. (a) Transmission electron micrograph (TEM) of an assembly of 16 layers: 8 CdSe quantum dots (QDs) alternating with 8 cross-linked polystyrene layers, assembled on a silicon wafer. Each bilayer is numbered on the micrograph from 1 to 8. In all the micrographs, a gold layer was sputtered on the film after fabrication to mark the air interface and masks the uppermost quantum dot layer. (b) A six-layer asembly made by assembling QDs and polystyrene (layer 1), pure polystyrene (layer 2), QDs and polystyrene (layer 3), and finally pure polystyrene (layer 4). The inset shows a TEM micrograph of the first layer normal to the substrate surface demonstrating a reasonably uniform film (c). Assembly of eight layers: four QDs and four polystyrene where the quantum dot layers are thicker than previous assemblies and the polystyrene are thinner (both ~15 nm).

tion, other enthalpic terms play an important role for these systems. Dispersion of CdSe quantum dots in nonpolar polystyrene is made possible by attachment of oleic acid chains to the quantum dot surfaces to yield a sterically stabilized system that is soluble in toluene. The quantum dots were synthesized using a previously published procedure[32] that involves injection of a selenium−trioctylphosphine solution into a heated (250 °C) CdO−oleic acid−heat transfer fluid solution and allowing the reaction to progress for ca. 1 h. Phase segregation of the quantum dots from linear polystyrene, in thin films, is clearly evident in transmission electron microscopy (TEM) images shown in Figure 2. We note that these quantum dots are completely soluble in bulk polystyrene, as occurs for others systems where nanoparticle architecture enables bulk miscibility, with a particularly notable case being dendritic polyethylene[33] in polystyrene.[24]

The TEM image in Figure 2a shows eight bilayers self-assembled with the SAMON process (Figure 1c) using the same linear polystyrene as above, having 20 mol % BCB groups that can be cross-linked. Each quantum dot layer is close to a monolayer coverage (approximately ~5 nm thick), and the thickness of each polymer layer is about 75 nm.

The quantum dots primarily assemble at the air interface in this system with the exception of the first layer, layer 1 in the figure, where they are at both interfaces. This is made clear by viewing Figure 2b, which has the following layer deposition scheme: layer 1, polymer + quantum dots; layer 2, pure polymer; layer 3, polymer + quantum dots; layer 4, pure polymer. Each layer is processed by thermal aging after spin coating to activate the cross-linking process before the subsequent layer is deposited. Some quantum dots have assembled at the substrate interface in layer 1, yet most have segregated to the air interface. This is more evident by viewing the interface between layers 2 and 3 and 3 and 4. Here it is clear that the quantum dots in layer 3 have mostly gone to the air interface which is subsequently covered by a pure, cross-linked polymer layer.

The assembly is easily described by careful consideration of the Hamaker constant for trilayers making-up a multilayer assembly. If the constant is negative, then that trilayer is stable with the effective interface potential positive to ensure stability.[34] If we consider a trilayer of air (component 1)−quantum dots (3)−polystyrene (2), then one can determine the sign of the Hamaker constant (A_{132}) using,[35] $A_{132} \sim [n_1^2 - n_3^2][n_2^2 - n_3^2]$, which is a good heuristic for nonconducting materials. Here n_i is the refractive index of component i with the following approximate values: 1.0 (air), 1.54 (quantum dots), and 1.59 (polystyrene). The value for the quantum dots' refractive index was arrived at by computing a volume average of a CdSe inner core with a 2.2 nm radius (refractive index of 2.8) surrounded by an oleic acid layer which is 2.5 nm thick (refractive index of 1.4). The oleic acid layer thickness was determined by dynamic light scattering of a dilute toluene solution and is a reasonable value based on the chemical structure. With these values,

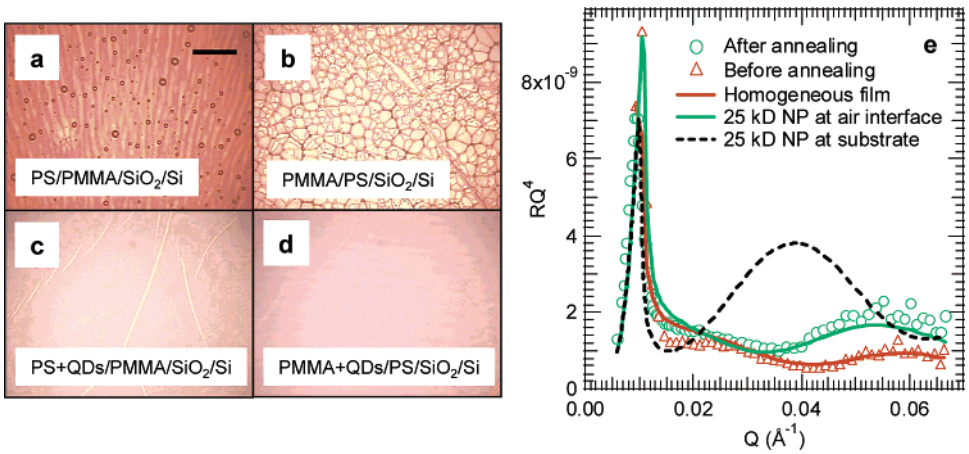

Figure 3. (a) Optical micrographs of a 58 nm thick polystyrene (PS) film floated onto a 56 nm thick PMMA film after thermal aging on a silicon (Si) wafer with its native oxide layer (SiO_2). Isolated polystyrene drops can be seen on the surface of PMMA. (b) PMMA film floated on polystyrene subject to the same annealing procedure given in (a) to show a similarly unstable film. The instabilities shown in (a) and (b) disappear in (c) and (d), respectively, when the top layer is replaced by a composite film composed of both the quantum dots (QDs) and the polymer. The film ordering is given in the figure with the abbreviations listed above; the length of the scale bar is 200 μm. (e) Reflectivity profile of 25 kDa nanoparticles (NPs) blended with 60 kDa partially deuterated NPs shows that before annealing the film is homogeneous while after thermal annealing the 25 kDa NPs assemble at the air interface rather than at the substrate.

the ordering of air−quantum dots−polystyrene is stable while others are not.

Of course, this type of assembly requires similar forces as described by Gupta et al.[31] However, since the nanoparticles are presumably homogeneously dispersed after the initial spin-coating step, they must rapidly diffuse to form the stable configuration before dewetting occurs. By use of the Stokes−Einstein relation and the viscosity for the polystyrene melt,[36] a diffusion coefficient of ca. 50 nm^2/s is calculated. Since the layer thickness is of order 50 nm, then approximately 1 min is required for the nanoparticles to diffuse to either interface. This time scale is so small that we believe the dewetting behavior is stabilized throughout the diffusion process as nanoparticles rapidly accumulate to their stable configuration thereby prohibiting nucleation and growth of holes. Nevertheless, some nanoparticles are trapped at the unstable position, for example near the substrate, either due to the entropic stabilization or by kinetic means where local cross-linking confines them at the given position. This later hypothesis seems unlikely since we have not observed quantum dots trapped in the middle of the film (Figure 2b).

Much thicker quantum dot layers and thinner polymer layers can also be formed as demonstrated in Figure 2c where ca. 15 nm thick quantum dot layers have been assembled with ~15 nm thick cross-linked polystyrene. Again, the first layer shows a thin quantum dot layer at the substrate with most of them located at the upper part of this film. Subsequent films show alternating layers of the two components which are not as coherent as the layers formed with a lesser amount of quantum dots, parts a and b of Figure 2 as well as the inset of Figure 2b, although they are certainly distinct. We believe the layers can be further refined through optimization of the processing conditions.

Generalization of the SAMON technique to incompatible, non-cross-linked polymers, and nanoparticles is demonstrated in Figure 3 where optical micrographs of PMMA and polystyrene polymers are considered. The first layer, either PMMA (76 kDa, Figure 3a) or polystyrene (75 kDa, Figure 3b), was spin-coated onto the silicon wafer, which has its native oxide layer, followed by floating the other polymer on top and aging the composite for 24 h at 180 °C. Both systems were found to dewet as expected; however, when the top layer contained quantum dots, the dewetting was eliminated as shown in parts c and d of Figure 3. Previous work has demonstrated that other nanoparticles will slow the dewetting dynamics;[37] however, our work shows complete elimination of dewetting. So, the SAMON process applies to a wide range of polymers, and stabilization may be carried out both with or without cross-linking the polymer layer yielding a robust procedure for self-assembly of functional multilayers from nonpolar nanoparticles and polymers.

We also show that the process can be extended to different sized nanoparticles[38] in Figure 3e. A blend of two cross-linked polystyrene nanoparticles, differing in molecular size, was spin-coated together on a silicon wafer at an overall and relative concentration to yield a monolayer of the larger nanoparticles and a bilayer of the smaller. One component was a cross-linked random copolymer of 80 mol % styrene−20 mol % BCB to form a nanoparticle (25 kDa molecular mass, radius ~2.3 nm) while the other nanoparticle had four styrene monomer units deuterated and the final BCB unit remained hydrogenated (60 kDa molecular mass, radius ~3.1 nm). Thermal aging was performed, and it was found that the larger nanoparticles segregated to the solid substrate in agreement with recent simulations.[39] This effect is caused by a system entropy gain since there are fewer larger particles near the wall per unit volume and hence less translational entropy loss for the system occurs as a whole. We tried another size ratio of nanoparticles, 3.1 and 4.1 nm radius, without significant success. A slight change in the homogeneous neutron reflectivity profile is seen after high-temperature aging, yet the difference is within experimental error and so delicate packing effects are apparent or the

nanoparticles are in a jammed state. Rheological characterization shows the two larger size nanoparticle systems (3.1 and 4.1 nm radius) have a yield stress while the smallest system (2.3 nm radius) does not,[21] which may trap the system into a kinetically stabilized state. Regardless we have developed a process to produce assembly on the nanoscale based on size dissimilarity as well as architecture.

Acknowledgment. This research was supported through NSF CTS-0400840, NSF NIRT-0210247, NSF−CTS-0417640, NSF NIRT-0506309, NSF DMR-0520415, DE-FG02-90ER45418, DE-FG02-05ER46211, ARO W911NF-05-1-0357, and also support by the U.S. Department of Energy, BES-Materials Science, under Contract W-31-109-ENG-38 to the University of Chicago is greatly appreciated as was the help of Dr. Pappannan Thiyagarajan, Denis Wozniak, and developers of data reduction routines at Argonne National Laboratory in gathering and analyzing the neutron scattering data. M.S.W. would like to acknowledge support from Advanced Aromatics and 3M Non-tenured Faculty Award.

References

(1) Huang, C. H.; McClenaghan, N. D.; Kuhn, A.; Bravic, G.; Bassani, D. M. *Tetrahedron* **2006**, *62*, 2050.
(2) Bagkar, N.; Betty, C. A.; Hassan, P. A.; Kahali, K.; Bellare, J. R.; Yakhmi, J. V. *Thin Solid Films* **2006**, *497*, 259.
(3) Bertolo, J. M.; Bearzotti, A.; Falcaro, P.; Traversa, E.; Innocenzi, P. *Sens. Lett.* **2003**, *1*, 64.
(4) Pages, X.; Rouessac, V.; Cot, D.; Nabias, G.; Durand, J. *Sep. Purif. Technol.* **2001**, *25*, 399.
(5) Ulbricht, M. *Polymer* **2006**, *47*, 2217.
(6) Lin, Y.; Skaff, H.; Emrick, T.; Dinsmore, A. D.; Russell, T. P. *Science* **2003**, *299*, 226.
(7) Lin, Y.; Boker, A.; He, J. B.; Sill, K.; Xiang, H. Q.; Abetz, C.; Li, X. F.; Wang, J.; Emrick, T.; Long, S.; Wang, Q.; Balazs, A.; Russell, T. P. *Nature* **2005**, *434*, 55.
(8) Lopes, W. A.; Jaeger, H. M. *Nature* **2001**, *414*, 735.
(9) Blodgett, K. B. *J. Am. Chem. Soc.* **1935**, *57*, 1007.
(10) Decher, G. *Science* **1997**, *277*, 1232.
(11) Cui, T. H.; Hua, F.; Lvov, Y. *Sens. Actuators, A* **2004**, *114*, 501.
(12) Tang, Z. Y.; Kotov, N. A.; Magonov, S.; Ozturk, B. *Nat. Mater.* **2003**, *2*, 413.
(13) Sellinger, A.; Weiss, P. M.; Nguyen, A.; Lu, Y. F.; Assink, R. A.; Gong, W. L.; Brinker, C. J. *Nature* **1998**, *394*, 256.
(14) Murahashi, T.; Fujimoto, M.; Oka, M.-a.; Hashimoto, Y.; Uemura, T.; Tatsumi, Y.; Nakao, Y.; Ikeda, A.; Sakaki, S.; Kurosawa, H. *Science* **2006**, *313*, 11.
(15) Huang, J. X.; Kim, F.; Tao, A. R.; Connor, S.; Yang, P. D. *Nat. Mater.* **2005**, *4*, 896.
(16) Bigioni, T. P.; Lin, X. M.; Nguyen, T. T.; Corwin, E. I.; Witten, T. A.; Jaeger, H. M. *Nat. Mater.* **2006**, *5*, 265.
(17) Stratford, K.; Adhikari, R.; Pagonabarraga, I.; Desplat, J. C.; Cates, M. E. *Science* **2005**, *309*, 2198.
(18) Adams, M.; Dogic, Z.; Keller, S. L.; Fraden, S. *Nature* **1998**, *393*, 349.
(19) Krishnan, R. S.; Mackay, M. E.; Hawker, C. J.; Van Horn, B. *Langmuir* **2005**, *21*, 5770.
(20) Harth, E.; VanHorn, B.; Lee, V. Y.; Germack, D. S.; Gonzales, C. P.; Miller, R. D.; Hawker, C. J. *J. Am. Chem. Soc.* **2002**, *124*, 8653.
(21) Tuteja, A.; Mackay, M. E.; Hawker, C. J.; VanHorn, B.; Ho, D. L. *J. Polym. Phys.: Polym. Phys.* **2006**, *44*, 1930−1947.
(22) Hariharan, A.; Kumar, S. K.; Rusell, T. P. *Macromolecules* **1990**, *23*, 3584.
(23) Jones, R.; Kumar, S.; Ho, D.; Briber, R.; Russell, T. *Macromolecules* **2001**, *34*, 559.
(24) Mackay, M. E.; Tuteja, A.; Duxbury, P. M.; Hawker, C. J.; Van Horn, B.; Guan, Z. B.; Chen, G. H.; Krishnan, R. S. *Science* **2006**, *311*, 1740.
(25) Yethiraj, A. *Phys. Rev. Lett.* **1995**, *74*, 2018.
(26) Lee, J. Y.; Buxton, G. A.; Balazs, A. C. *J. Chem. Phys.* **2004**, *121*, 5531.
(27) Tyagi, S.; Lee, J. Y.; Buxton, G. A.; Balazs, A. C. *Macromolecules* **2004**, *37*, 9160.
(28) Barnes, K. A.; Douglas, J. F.; Liu, D. W.; Karim, A. *Adv. Colloid Interface Sci.* **2001**, *94*, 83.
(29) Barnes, K. A.; Karim, A.; Douglas, J. F.; Nakatani, A. I.; Gruell, H.; Amis, E. J. *Macromolecules* **2000**, *33*, 4177.
(30) Mackay, M. E.; Hong, Y.; Jeong, M.; Hong, S.; Russell, T. P.; Hawker, C. J.; Vestberg, R.; Douglas, J. F. *Langmuir* **2002**, *18*, 1877.
(31) Gupta, S.; Zhang, Q. L.; Emrick, T.; Balazs, A. C.; Russell, T. P. *Nat. Mater.* **2006**, *5*, 229.
(32) Asokan, S.; Krueger, K. M.; Alkhawaldeh, A.; Carreon, A. R.; Mu, Z. Z.; Colvin, V. L.; Mantzaris, N. V.; Wong, M. S. *Nanotechnology* **2005**, *16*, 2000.
(33) Guan, Z.; Cotts, P.; McCord, E.; McLain, S. *Science* **1999**, *283*, 2059.
(34) Seemann, R.; Herminghaus, S.; Neto, C.; Schlagowski, S.; Podzimek, D.; Konrad, R.; Mantz, H.; Jacobs, K. *J. Phys.: Condens. Mater.* **2005**, *17*, S267.
(35) Israelachvili, J. N. *Intermolecular and Surface Forces*; Academic Press: New York, 1992.
(36) Fox, T. G.; Flory, P. J. *J. Am. Chem. Soc.* **1948**, *70*, 2384.
(37) Xavier, J. H.; Sharma, S.; Seo, Y. S.; Isseroff, R.; Koga, T.; White, H.; Ulman, A.; Shin, K.; Satija, S. K.; Sokolov, J.; Rafailovich, M. H. *Macromolecules* **2006**, *39*, 2972.
(38) Zeng, H.; Li, J.; Liu, J. P.; Wang, Z. L.; Sun, S. H. *Nature* **2002**, *420*, 395.
(39) Roth, R.; Dietrich, S. *Phys. Rev. E* **2000**, *62*, 6926.

NL062866U